IOP Publishing Environ. Res. Lett. 18 (2023) 044027 https://doi.org/10.1088/1748-9326/acc676

ENVIRONMENTAL RESEARCH
LETTERS

OPEN ACCESS

RECEIVED
29 August 2022

REVISED
6 March 2023

ACCEPTED FOR PUBLICATION
22 March 2023

PUBLISHED
4 April 2023

LETTER

Moisture origins of the Amazon carbon source region

Arie Staal[1,*], **Gerbrand Koren**[1], **Graciela Tejada**[2] **and Luciana V Gatti**[2,3]

[1] Copernicus Institute of Sustainable Development, Utrecht University, Utrecht, The Netherlands
[2] General Coordination of Earth Science (CGCT), National Institute for Space Research (INPE), São José dos Campos, Brazil
[3] Nuclear and Energy Research Institute (IPEN), São Paulo, Brazil
[*] Author to whom any correspondence should be addressed.

E-mail: a.staal@uu.nl

Keywords: climate change, carbon sink, atmospheric moisture recycling, tropics

Supplementary material for this article is available online

Abstract

The southeastern Amazon has recently been shown to be a net carbon source, which is partly caused by drying conditions. Drying depends on a number of factors, one of which is the land cover at the locations where the moisture has originated as evaporation. Here we assess for the first time the origins of the moisture that precipitates in the Amazon carbon source region, using output from a Lagrangian atmospheric moisture tracking model. We relate vegetation productivity in the Amazon carbon source region to precipitation patterns and derive land-cover data at the moisture origins of these areas, allowing us to estimate how the carbon cycle and hydrological cycle are linked in this critical part of the Amazon. We find that, annually, 13% of the precipitation in the Amazon carbon source region has evaporated from that same area, which is half of its land-derived moisture. We further find a moisture-recycling-mediated increase in gross primary productivity of roughly 41 Mg carbon km^{-2} yr^{-1} within the Amazon carbon source region if it is fully forested compared to any other land cover. Our results indicate that the parts of the Amazon forest that are already a net carbon source, still help sustain their own biomass production. Although the most degraded parts of the Amazon depend mostly on oceanic input of moisture, further degradation of this region would amplify carbon losses to the atmosphere.

1. Introduction

Earth's biosphere is currently a net carbon sink that stabilizes the climate, and maintaining this sink is key to prevent catastrophic climate change [1]. Among the greatest threats to the global climate is the possibility that the Amazon rainforest, Earth's largest aboveground carbon stock [2], becomes a net carbon source [3, 4]. This would set in motion a positive feedback with global mean temperature that amplifies global warming [5, 6]. To assess the state of the Amazon's carbon budget, Gatti *et al* [7] performed 590 atmospheric vertical profiling measurements from four sites using aircraft over the course of nine years (2010–2018). They found that intact forests of the southeastern Amazon already act as a carbon source, fuelling fears that the Amazon as a whole will flip from net sink to net source as global climate change continues [4]. Whether this will occur depends critically on precipitation levels: both intensifying seasonal droughts and increasingly recurring severely dry years may cause this flip to happen [4, 8, 9]. However, importantly, precipitation levels are not beyond human influence. Generally, precipitation over land originates partly from ocean and partly from land [10, 11]. The land-derived component of precipitation and its variability depend on land cover at its source of evapotranspiration [12]. Specifically, tropical forests tend to produce a larger flux of evapotranspiration than pastures or grasslands, especially in the dry season when their deeper roots allow them to access deeper groundwater [13]. Likewise, different crops and different means of irrigation may produce different moisture fluxes from the land to the atmosphere. Therefore, land-cover changes such as reforestation could significantly enhance precipitation levels [14, 15].

The spatial connection between evapotranspiration and precipitation implies a causal link between land cover and the carbon budget at remote locations.

Due to recent advances in atmospheric moisture tracking [11, 16], it has become possible to obtain such connections at high spatial and temporal detail. Together with the vertical-profiling measurements by Gatti *et al* [7], this means that it is now possible to obtain the seasonally changing spatial distributions of the moisture origins of those parts of the Amazon that are at critical need of moisture to maintain or regain their function as net carbon sink (or at least be carbon neutral). Here we map those moisture origins for different parts of the Amazon with varying carbon dynamics as identified by Gatti *et al* [7], with a focus on the moisture origins of the region in the Amazon that is identified as net carbon source. We obtain land characteristics of these areas to explore the potential to restore the ecosystem service of remote moisture provisions.

2. Methods

2.1. Definition of the regions of influence

We use the mean regions of influence of each quarter for the period 2010–2018, based on all vertical profiles that were collected twice a month from airplanes by Gatti *et al* [7, 9]. The regions of influence were calculated using the HYSPLIT model [17] which uses individual back trajectories for each flask (height) of each vertical profile at 1 h resolution to get the trajectory density (number of back trajectories over a $1^\circ \times 1^\circ$ grid cell). Detailed methods of the region of influence calculations are found in Cassol *et al* [18], Gatti *et al* [7], and Basso *et al* [19]. These regions of influence correspond to the southeastern region ALF, southwestern region RBA, northeastern region SAN, and the northwestern region TAB (2010–2012) and TEF (2013–2018). We also refer to ALF as the Amazon carbon source region.

2.2. Atmospheric moisture tracking

To identify moisture origins of precipitation, we use the Lagrangian atmospheric moisture tracking model UTrack [16] to track the origins of precipitation backward in time. The model tracks the atmospheric trajectories of moisture parcels and updates their coordinates in three-dimensional space. For each mm of precipitation in an area of interest (here, the regions of influence), 100 parcels are released into the atmosphere. Their trajectories are forced with three-dimensional hourly wind speed estimates from the ERA5 reanalysis product at 0.25° horizontal resolution for 25 atmospheric layers [20]. Every time step, here 0.25 h, the moisture content of each parcel is updated depending on ERA5 evaporation data, in which case the evaporated amount of moisture, tracked backward from its location of precipitation, is allocated to the current position of the parcel. Also every time step, parcels have a certain probability of being assigned a new vertical position. This happens such that on average every 24 h each parcel is repositioned, the altitude of which depends on the vertical moisture profile. A parcel is no longer tracked after 30 days or when 99% of its original moisture has been allocated to evaporation. We store results for each region of influence and for each month during 2010–2018 and summed these monthly moisture flows for each quarter of the year. For further details of the UTrack model, we refer to Tuinenburg and Staal [16].

We define the land precipitation recycling ratio ρ_{land} of a particular region as the percentage of its precipitation that has last evaporated from land. For these additional results, we use the UTrack runs from Tuinenburg *et al* [11] resulting in monthly climatological mean (2008–2017) moisture flows between each pair of 0.5° grid cells across the globe. We define the region-of-influence precipitation recycling ratio ρ_{ROI} as the percentage of precipitation within a certain region of influence that has last evaporated within the same region of influence. We calculate these statistics for each of the regions of influence defined by Gatti *et al* [7].

Note that the model we use to simulate the trajectories of moisture fluxes is different than the model used by Gatti *et al* [7, 9] to simulate the backward trajectories or the regions of influence.

2.3. Evapotranspiration and precipitation

To maintain consistency with the atmospheric moisture tracking results, we use the ERA5 global reanalysis dataset for all precipitation and evapotranspiration estimates [20]. Furthermore, to estimate the contribution of forest cover to evapotranspiration at the moisture origins, we use the calculations by Tuinenburg *et al* [15]. They applied the global hydrological model PCR-GLOBWB [21, 22], simulated for 1981–2010, to determine, globally and for each 0.5° grid cell and month, the evapotranspiration difference between a fully covered forest and the highest-evaporating alternative land cover (natural grassland, pasture, or cropland).

2.4. Gross primary productivity

We obtained monthly gross primary productivity (GPP) data at 0.05° resolution for ALF during 2010–2018 from Wang *et al* [23]. This product is based on near-infrared reflectance of vegetation (NIRv) that was first described by Badgley *et al* [24] as a robust proxy for GPP. Furthermore, the GPP product [23] that we use here was found to be close to the median in a recent systematic assessment of eight GPP products [25]. Although higher-resolution datasets exist (such as MapBiomas or ESA CCI Land Cover), 0.05° is more than enough for our purpose, for which we need land cover fractions at 0.25° resolution. As a first-order estimate of the effect of precipitation on GPP, we performed a linear regression of monthly GPP in ALF to precipitation. Because the region

of influence ALF varies throughout the year due to seasonal changes in winds [7], we first normalized GPP to a consistent unit of MgC km^{-2} month^{-1}. Combined with the estimated effect of forest cover on evapotranspiration in ALF [15], and the evaporation recycling ratio for ALF, we compute for ALF how much additional GPP during a given period would result from forest cover increase in ALF itself:

$$\Delta \mathrm{GPP}_{\mathrm{ALF}} = \mathrm{ET}_{\mathrm{forest,\ ALF}} \cdot \rho_{\mathrm{ET,ALF}} \cdot \frac{\mathrm{dGPP}_{\mathrm{ALF}}}{\mathrm{dP}_{\mathrm{ALF}}} \quad (1)$$

where $\Delta \mathrm{GPP}_{\mathrm{ALF}}$ is the increase in gross primary productivity (kgC over time), $\mathrm{ET}_{\mathrm{forest,ALF}}$ (mm over time) is the evapotranspiration by forest cover within ALF, $\rho_{\mathrm{ET,ALF}}$ (fraction) is the evaporation recycling ratio for ALF, and $\mathrm{dGPP}_{\mathrm{ALF}}/\mathrm{d}P_{\mathrm{ALF}}$ (kgC mm^{-1}) is the slope of GPP as a function of precipitation.

2.5. Land cover classes

We determined statistics of the land cover at the moisture origins of ALF. For this we used the MODIS MCD12C1 version 6.1 dataset at 0.05° resolution for the year 2018 [26]. We used the International Geosphere-Biosphere Programme layer, which we simplified to six land-cover classes: forest (evergreen needleleaf forest, evergreen broadleaf forest, deciduous needleleaf forest, deciduous broadleaf forest, and mixed forests), shrubland (closed shrubland and open shrubland), savanna (woody savannas and savannas), grassland, cropland (croplands and cropland/natural vegetation mosaic), and other (urban and built up, and barren or sparsely vegetated). We weighted the contribution of the land covers by the evaporation that they contribute to precipitation in ALF. In this way, we obtained a relative measure (in percentage) of the contributions of moisture from these different land cover classes to the Amazon carbon source region.

3. Results

We focus on the southeastern portion of the Amazon rainforest, the region of influence of the aircraft's vertical profiling site at ALF, as this region was found to be a net carbon source. ALF received an average of 488 mm (±47 mm standard deviation among years) precipitation per year from local and surrounding land areas during 2010–2018 (figures 1 and S2; table 1). Given its mean annual average precipitation of 1919 mm, the majority (75%) of precipitation in ALF has oceanic origin. Out of the land-originated precipitation, 52% (253 ± 27 mm) has evaporated within ALF itself, with the remainder originating from more eastern land areas. Most of this terrestrial moisture comes from Brazil (figure 1). Switching the perspective to evapotranspiration instead of precipitation, we find that 24% of all evaporation from ALF is recycled within ALF itself.

We find seasonality in the amount of moisture that is recycled within ALF as well as that imported from other land areas (figures 1 and S1; table 1). The region of influence was separated by Gatti *et al* [7] for the four quarters of the calendar year. In the first quarter, on average 12% (117 ± 11 mm) of the precipitation comes from within ALF and 21% (204 ± 18 mm) from land; in the second quarter, 10% (34 ± 4 mm) of the precipitation comes from ALF and 28% (97 ± 12 mm) from land; in the third quarter, 12% (7 ± 5 mm) of the precipitation comes from ALF and 25% (14 ± 10 mm) from land; finally, in the fourth quarter, 16% (90 ± 22 mm) the comes from ALF and 33% (179 ± 37 mm) from land (table 1). Thus, in absolute terms, recycling within ALF peaks in the first quarter, but in relative terms in the fourth quarter. Although total recycling is relatively low during the driest months (third quarter), mainly due to the relatively large contribution of Amazonian trees to evapotranspiration when it is drier, recycling of the moisture that has been transpired by trees is relatively high in the dry season [13]. Note that the shape and size of the regions of influence are different for each quarter. Moisture recycling ratios tend to be higher for larger areas [11, 27, 28] and the regions of influence are indeed smaller in the second and third quarters (0.9×10^6 km^2 and 1.0×10^6 km^2) than in the first and fourth ones (1.7×10^6 km^2 and 1.6×10^6 km^2) (figure 1).

The fact that ALF has a history of land-use change means that the estimated local dependency on moisture may be lower than it used to be, but also suggests that there could be potential to restore it. Therefore, we determined the land cover at the origins of the moisture flows to ALF. We find that forest occupied on average 46% of the terrestrial origins, savanna 34%, grassland 16%, cropland 2%, shrubland 1%, and all other land covers (such as urban areas) a negligible amount. The large proportion of natural areas (both forest and savanna) suggests that maintaining as much moisture flow towards ALF would primarily involve conserving existing ecosystems. This is further confirmed by a recent study [29] showing the largest climate benefits in Brazil would be achieved by conserving existing forests. Still, a larger carbon stock in ALF, including secondary forests and other vegetation, would benefit the carbon sink there [30].

Although a positive effect of precipitation on the carbon sink is to be expected in the ALF region of influence, it is less obvious what that relation looks like. Therefore, we took the monthly GPP in ALF (mean = 0.27 GgC km^{-2} month^{-1}) and related that to monthly precipitation (during 2010–2018). A linear regression fits reasonably well (R^2 = 0.54; figure 2), in which every mm of monthly precipitation tends to increase GPP by 0.22 MgC km^{-2} month^{-1}. The residual standard

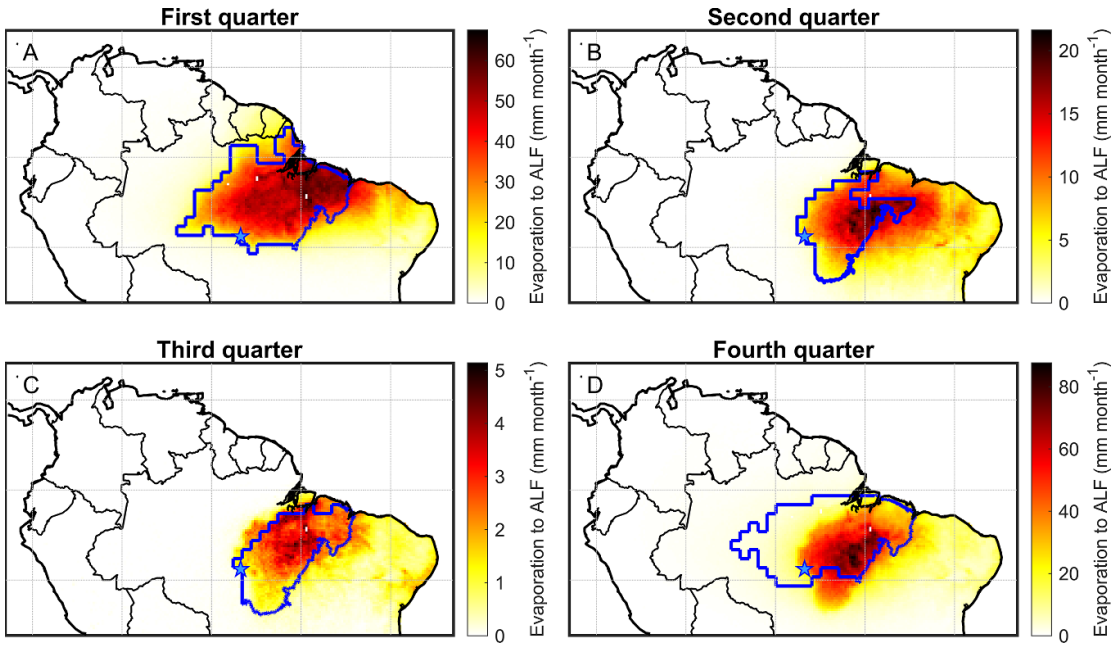

Figure 1. Average (2010–2018) land evaporation (mm month^{-1}) in each quarter that precipitates in the Amazonian southeast ALF, the part of the Amazon that has been found to be a carbon source. The boundaries of the regions of influence of the vertical profiling measurements [7] are given in blue, which means that the definition of ALF is different for each quarter. The location of the ALF vertical profiling measurements is depicted with the blue star. Note the different colour scales across the plots. For the figures of the other subregions, of which the intact forests are found to still be a net carbon sink, see the supplementary figures S2–S5.

Table 1. Annual and quarterly precipitation (P, in mm), land precipitation recycling ratio (ρ_{land}, in %), and precipitation recycling ratio of ALF (ρ_{ALF}, in %). Between brackets are the standard deviations (all based on the period 2010–2018). For results of all regions of influence, see table S1.

	Annual	Q1	Q2	Q3	Q4
P (mm)	1919 (±162)	967 (±94)	344 (±38)	58 (±33)	550 (±102)
ρ_{land} (%)	25 (±2)	21 (±2)	28 (±4)	25 (±17)	33 (±7)
ρ_{ALF} (%)	13 (±1)	12 (±1)	10 (±1)	12 (±9)	16 (±4)

deviation is 0.026 GgC km^{-2} month^{-1}. Forest cover in ALF is estimated to increase evapotranspiration rates by at least 81 mm month^{-1} on average: 71 mm month^{-1} in the first quarter, 70 mm month^{-1} in the second quarter, 85 mm month^{-1} in the third quarter, and 98 mm month^{-1} in the fourth quarter. In the first quarter, 37% of the evapotranspiration in ALF returns as precipitation in ALF; in the second quarter, this is 11%, in the third quarter it is 3%, and in the fourth quarter 27%. This means that a fully covered forest in ALF enhances precipitation by 26 mm month^{-1}, 8 mm month^{-1}, 2 mm month^{-1}, and 26 mm month^{-1} in the respective quarters. This sums to 186 mm yr^{-1}, which translates into an estimated 41 MgC km^{-2} of additional GPP annually. There are reasons, however, to assume that this value is an underestimation. Namely, it disregards the strongly nonlinear effect that forest cover increase may have on precipitation [31]. Furthermore, the intercept in figure 2 implies that 0.23 GgC km^{-2} month^{-1} is produced at 0 mm precipitation, which is not realistic. It should also be noted that the moisture-recycling-mediated effect is not the only biophysical effect that forest change has on productivity [32] and that we focus here on dynamics within the Amazon carbon source region only.

We present the moisture-recycling results for all regions of influence in the supplementary figures S2–S5 and table S1. Although mean annual precipitation varies only little among regions of influence (1900–2148 mm yr^{-1}), the precipitation recycling ratios vary considerably: lowest annual ρ_{land} is found for SAN (northeast) with only 13% and highest for RBA (southeast) with 31%. Both in absolute amounts and relative amounts of moisture recycling, and both on an annual basis and peak-quarterly basis (fourth quarter), both ρ_{land} and ρ_{ROI} are highest in RBA (table S1).

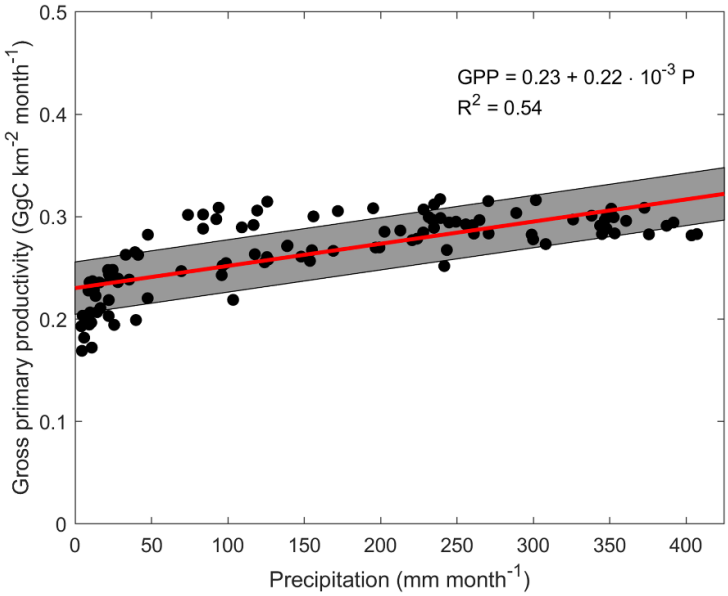

Figure 2. Gross primary productivity (GPP, in GgC km^{-2} month^{-1}) in ALF as a function of precipitation (P in mm month^{-1}) for each month during 2010–2018. GPP is normalized to km^{-2} because of the differing area of the ALF region of influence throughout the year. The grey band represents one standard deviation around the linear fit ($R^2 = 0.54$; $p \ll 0.01$).

4. Discussion

We present the moisture origins of the carbon source region in the southeastern Amazon, highlighting where forest conservation and restoration may contribute to prevent further carbon emissions or restore the carbon sink. We add to previous work about the role of forest in generating precipitation in the (southern) Amazon (e.g.) [13, 33–40] by specifically targeting the area that was identified by Gatti *et al* [7] as a carbon source. We find that 13% of its precipitation has originated from within the same region, indicating a regional positive feedback between GPP and precipitation.

Positive (reinforcing) feedbacks are ubiquitous in tropical forests [41] and can cause tipping points [42], which present a possible threat to the Amazon [6, 43, 44]. An example of such a positive feedback exists between fire and tree cover loss, which could trap a landscape in a state of low tree cover maintained by fire [45–47]. Regionally, forests enhance precipitation, feeding back to the forest [13]. The positive feedback between CO_2 concentrations and temperature is global, so the effects of enhanced carbon fluxes from the forest to the atmosphere are spread out globally. As this would be unlikely to cause runaway global warming by itself, it cannot be concluded that a tipping point is reached once ALF (or even the Amazon as a whole) becomes a net carbon source. Still, reduced photosynthesis is causally coupled to reduced moisture transport from the soil to the atmosphere. Thus, lowered primary productivity reduces atmospheric moisture recirculation, which implies a weakening of the positive forest-precipitation feedback that is crucial to parts of the Amazon. The finding that a significant part (249 mm, or 13%) of the annual precipitation in the Amazon's carbon source region has last evaporated within the same area suggests the potential for a destabilizing (positive) feedback within the subregion if drought conditions worsen. Indeed, self-amplifying tipping points are found to be most likely in the southeastern forests of the Amazon, regardless of whether absolute climatic tipping points are assumed [43] or whether tipping points relative to local climatic history are assumed [48].

We have assessed nearly a decade of carbon exchange and moisture flows in the Amazon. This period contains not only seasonal variations but also substantial interannual variations, with some notable wet and dry years. These include the extremely dry years 2010 [49] and 2015/16 [50], which had major impacts on carbon cycling due to reduced photosynthesis and increased fires, as confirmed by vertical profiles [9], remote sensing [51, 52], and models [53]. In addition, the study period contains the wet years 2009 [54], 2012 [55], and 2014 [56]. However, despite the large interannual precipitation variability during the study period, the moisture flows within and to the Amazon carbon source region were robust (with standard deviations of around 10% of the interannual means). Therefore, we are confident that our derived estimates for moisture flows and the sensitivity of carbon uptake to precipitation are representative for a large range of conditions.

We based our analysis on the sensitivity of the carbon uptake on the regression between GPP and precipitation. We selected GPP for this analysis, because the assimilation of carbon through photosynthesis is the starting point for the subsequent carbon cycling

through the ecosystem, and is highly sensitive to environmental conditions. We acknowledge that this does not necessarily result in biomass production, as ecosystem respiration also varies with moisture and temperature (e.g.) [57], but this response is typically less strong [58]. Our results should thus be considered a first-order approximation to precipitation variability, and future work with dynamic vegetation models can provide more accurate results on the net carbon exchange of the ecosystem. Furthermore, uncertainties in the different measurements (such as the airborne measurements and related estimates of the regions of influence) and models (such as the UTrack moisture tracking model) that underlie our results may propagate. Future research should determine in more detail how forest loss or restoration may cascade through the Amazon forest system through moisture recycling and thus affect the carbon exchange between the forest and the atmosphere.

5. Conclusion

Our findings indicate that conservation of the Amazon carbon source region itself helps to maintain precipitation levels within the same region. More degradation of the forests may lead to a further reduction of the forest's ability to capture atmospheric CO_2 via reduced atmospheric moisture recycling, stressing the importance of conserving Amazonian forests to maintain Earth's terrestrial carbon sink.

Data availability statement

The data that support the findings of this study are openly available at the following URL/DOI: 10.5281/zenodo.7636227.

Acknowledgment

A S is supported by the Dutch Research Council (NWO) Talent Program Grant VI.Veni.202.170.

Code availability statement

Code for the UTrack model can be downloaded from https://github.com/ObbeTuinenburg/UTrackatmospheric-moisture.

ORCID iDs

Arie Staal https://orcid.org/0000-0001-5409-1436
Gerbrand Koren https://orcid.org/0000-0002-2275-0713

References

[1] Rockström J, Beringer T, Hole D, Griscom B, Mascia M B, Folke C and Creutzig F 2021 We need biosphere stewardship that protects carbon sinks and builds resilience *Proc. Natl Acad. Sci.* **118** e2115218118
[2] Saatchi S S *et al* 2011 Benchmark map of forest carbon stocks in tropical regions across three continents *Proc. Natl Acad. Sci.* **108** 9899–904
[3] Brienen R J W *et al* 2015 Long-term decline of the Amazon carbon sink *Nature* **519** 344–8
[4] Hubau W *et al* 2020 Asynchronous carbon sink saturation in African and Amazonian tropical forests *Nature* **579** 80–87
[5] Steffen W *et al* 2018 Trajectories of the Earth System in the Anthropocene *Proc. Natl Acad. Sci.* **115** 8252–9
[6] Armstrong McKay D I, Staal A, Abrams J F, Winkelmann R, Sakschewski B, Loriani S, Fetzer I, Cornell S E, Rockström J and Lenton T M 2022 Updated assessment suggests >1.5 °C global warming could trigger multiple climate tipping points *Science* **377** eabn7950
[7] Gatti L V *et al* 2021 Amazonia as a carbon source linked to deforestation and climate change *Nature* **595** 388–93
[8] Yang Y, Saatchi S S, Xu L, Yu Y, Choi S, Phillips N, Kennedy R, Keller M, Knyazikhin Y and Myneni R B 2018 Post-drought decline of the Amazon carbon sink *Nat. Commun.* **9** 3172
[9] Gatti L V *et al* 2014 Drought sensitivity of Amazonian carbon balance revealed by atmospheric measurements *Nature* **506** 76–80
[10] Van der Ent R J, Savenije H H G, Schaefli B and Steele-Dunne S C 2010 Origin and fate of atmospheric moisture over continents *Water Resour. Res.* **46** W09525
[11] Tuinenburg O A, Theeuwen J J E and Staal A 2020 High-resolution global atmospheric moisture connections from evaporation to precipitation *Earth Syst. Sci. Data* **12** 3177–88
[12] O'Connor J C, Dekker S C, Staal A, Tuinenburg O A, Rebel K T and Santos M J 2021 Forests buffer against variations in precipitation *Glob. Change Biol.* **27** 4686–96
[13] Staal A, Tuinenburg O A, Bosmans J H C, Holmgren M, van Nes E H, Scheffer M, Zemp D C and Dekker S C 2018 Forest-rainfall cascades buffer against drought across the Amazon *Nat. Clim. Change* **8** 539–43
[14] Hoek van Dijke A J, Herold M, Mallick K, Benedict I, Machwitz M, Schlerf M, Pranindita A, Theeuwen J J E, Bastin J-F and Teuling A J 2022 Shifts in regional water availability due to global tree restoration *Nat. Geosci.* **15** 363–8
[15] Tuinenburg O A, Bosmans J H C and Staal A 2022 The global potential of forest restoration for drought mitigation *Environ. Res. Lett.* **17** 034045
[16] Tuinenburg O A and Staal A 2020 Tracking the global flows of atmospheric moisture and associated uncertainties *Hydrol. Earth Syst. Sci.* **24** 2419–35
[17] Stein A F, Draxler R R, Rolph G D, Stunder B J B, Cohen M D and Ngan F 2015 NOAA's HYSPLIT atmospheric transport and dispersion modeling system *Bull. Am. Meteorol. Soc.* **96** 2059–77
[18] Cassol H L G *et al* 2020 Determination of region of influence obtained by aircraft vertical profiles using the density of trajectories from the HYSPLIT model *Atmosphere* **11** 1073
[19] Basso L S *et al* 2021 Amazon methane budget derived from multi-year airborne observations highlights regional variations in emissions *Commun. Earth Environ.* **2** 246
[20] Hersbach H *et al* 2020 The ERA5 global reanalysis *Q. J. R. Meteorol. Soc.* **146** 1999–2049
[21] Bosmans J H C, van Beek L P H, Sutanudjaja E H and Bierkens M F P 2017 Hydrological impacts of global land cover change and human water use *Hydrol. Earth Syst. Sci.* **21** 5603–26
[22] Sutanudjaja E H *et al* 2018 PCR-GLOBWB 2: a 5 arcmin global hydrological and water resources model *Geosci. Model Dev.* **11** 2429–53
[23] Wang S, Zhang Y, Ju W, Qiu B and Zhang Z 2021 Tracking the seasonal and inter-annual variations of global gross primary production during last four decades using satellite near-infrared reflectance data *Sci. Total Environ.* **755** 142569
[24] Badgley G, Field C B and Berry J A 2017 Canopy near-infrared reflectance and terrestrial photosynthesis *Sci. Adv.* **3** e1602244

[25] Dong J, Li L, Li Y and Yu Q 2022 Inter-comparisons of mean, trend and interannual variability of global terrestrial gross primary production retrieved from remote sensing approach *Sci. Total Environ.* **822** 153343
[26] Bonta M and Sulla-Menashe D 2015 MCD12C1 MODIS/terra+aqua land cover type yearly L3 global 0.05Deg CMG V006
[27] Molina R D, Salazar J F, Martínez J A, Villegas J C and Arias P A 2019 Forest-induced exponential growth of precipitation along climatological wind streamlines over the Amazon *J. Geophys. Res. Atmos.* **124** 2589–99
[28] Spracklen D V, Arnold S R and Taylor C M 2012 Observations of increased tropical rainfall preceded by air passage over forests *Nature* **489** 282−5
[29] Walker W S *et al* 2022 The global potential for increased storage of carbon on land *Proc. Natl Acad. Sci.* **119** e2111312119
[30] Heinrich V H A *et al* 2021 Large carbon sink potential of secondary forests in the Brazilian Amazon to mitigate climate change *Nat. Commun.* **12** 1785
[31] Baudena M, Tuinenburg O A, Ferdinand P A and Staal A 2021 Effects of land-use change in the Amazon on precipitation are likely underestimated *Glob. Change Biol.* **27** 5580–7
[32] Li Y, Brando P M, Morton D C, Lawrence D M, Yang H and Randerson J T 2022 Deforestation-induced climate change reduces carbon storage in remaining tropical forests *Nat. Commun.* **13** 1964
[33] Wright J S, Fu R, Worden J R, Chakraborty S, Clinton N E, Risi C, Sun Y and Yin L 2017 Rainforest-initiated wet season onset over the southern Amazon *Proc. Natl Acad. Sci.* **114** 8481–6
[34] Spracklen D V, Baker J C A, Garcia-Carreras L and Marsham J 2018 The effects of tropical vegetation on rainfall *Annu. Rev. Environ. Resour.* **43** 193–218
[35] Li W, Fu R and Dickinson R E 2006 Rainfall and its seasonality over the Amazon in the 21st century as assessed by the coupled models for the IPCC AR4 *J. Geophys. Res. Atmos.* **111** D02111
[36] Pires G F and Costa M H 2013 Deforestation causes different subregional effects on the Amazon bioclimatic equilibrium *Geophys. Res. Lett.* **40** 3618−23
[37] Costa M H and Pires G F 2010 Effects of Amazon and Central Brazil deforestation scenarios on the duration of the dry season in the arc of deforestation *Int. J. Climatol.* **30** 1970–9
[38] Nobre C A, Sampaio G, Borma L S, Castilla-Rubio J C, Silva J S and Cardoso M 2016 Land-use and climate change risks in the Amazon and the need of a novel sustainable development paradigm *Proc. Natl Acad. Sci.* **113** 10759−68
[39] Zemp D C, Schleussner C F, Barbosa H M J and Rammig A 2017 Deforestation effects on Amazon forest resilience *Geophys. Res. Lett.* **44** 6182–90
[40] Sampaio G, Nobre C, Costa M H, Satyamurty P, Soares-filho B S and Cardoso M 2007 Regional climate change over eastern Amazonia caused by pasture and soybean cropland expansion *Geophys. Res. Lett.* **34** L17709
[41] Flores B M and Staal A 2022 Feedback in tropical forests of the Anthropocene *Glob. Change Biol.* **28** 5041–61
[42] Van Nes E H, Arani B M S, Staal A, van der Bolt B, Flores B M, Bathiany S and Scheffer M 2016 What do you mean, 'tipping point'? *Trends Ecol. Evol.* **31** 902−4
[43] Zemp D C, Schleussner C F, Barbosa H M J, Hirota M, Montade V, Sampaio G, Staal A, Wang-Erlandsson L and Rammig A 2017 Self-amplified Amazon forest loss due to vegetation-atmosphere feedbacks *Nat. Commun.* **8** 14681
[44] Lovejoy T E and Nobre C 2018 Amazon tipping point *Sci. Adv.* **4** eaat2340
[45] Hirota M, Holmgren M, van Nes E H and Scheffer M 2011 Global resilience of tropical forest and savanna to critical transitions *Science* **334** 232−5
[46] Staver A C, Archibald S and Levin S A 2011 The global extent and determinants of savanna and forest as alternative biome states *Science* **334** 230–2
[47] Van Nes E H, Staal A, Hantson S, Holmgren M, Pueyo S, Bernardi R E, Flores B M, Xu C and Scheffer M 2018 Fire forbids fifty-fifty forest *PLoS One* **18** e0191027
[48] Wunderling N, Staal A, Sakschewski B, Hirota M, Tuinenburg O A, Donges J F, Barbosa H M J and Winkelmann R 2022 Recurrent droughts increase risk of cascading tipping events by outpacing adaptive capacities in the Amazon rainforest *Proc. Natl Acad. Sci.* **119** e2120777119
[49] Lewis S L, Brando P M, Phillips O L, van der Heijden G M F and Nepstad D 2011 The 2010 Amazon drought *Science* **331** 554
[50] Jiménez-Muñoz J C, Mattar C, Barichivich J, Santamaría-Artigas A, Takahashi K, Malhi Y, Sobrino J A and Schrier G V D 2016 Record-breaking warming and extreme drought in the Amazon rainforest during the course of El Niño 2015–2016 *Sci. Rep.* **6** 33130
[51] Koren G *et al* 2018 Widespread reduction in sun-induced fluorescence from the Amazon during the 2015/2016 El Niño *Phil. Trans. R. Soc.* B **373** 20170408
[52] Naus S *et al* 2022 Sixteen years of MOPITT satellite data strongly constrain Amazon CO fire emissions *Atmospheric Chem. Phys.* **22** 14735–50
[53] Van Schaik E, Killaars L, Smith N E, Koren G, van Beek L P H, Peters W and van der Laan-luijkx I T 2018 Changes in surface hydrology, soil moisture and gross primary production in the Amazon during the 2015/2016 El Niño *Phil. Trans. R. Soc.* B **373** 20180084
[54] Filizola N, Latrubesse E M, Fraizy P, Souza R, Guimarães V and Guyot J-L 2014 Was the 2009 flood the most hazardous or the largest ever recorded in the Amazon? *Geomorphology* **215** 99–105
[55] Satyamurty P, da Costa C P W, Manzi A O and Candido L A 2013 A quick look at the 2012 record flood in the Amazon Basin *Geophys. Res. Lett.* **40** 1396–401
[56] Espinoza J C, Marengo J A, Ronchail J, Carpio J M, Flores L N and Guyot J L 2014 The extreme 2014 flood in south-western Amazon basin: the role of tropical-subtropical South Atlantic SST gradient *Environ. Res. Lett.* **9** 124007
[57] Flanagan L B and Johnson B G 2005 Interacting effects of temperature, soil moisture and plant biomass production on ecosystem respiration in a northern temperate grassland *Agric. For. Meteorol.* **130** 237–53
[58] Piao S, Wang X, Wang K, Li X, Bastos A, Canadell J G, Ciais P, Friedlingstein P and Sitch S 2020 Interannual variation of terrestrial carbon cycle: issues and perspectives *Glob. Change Biol.* **26** 300–18